NASA CONTRACTOR REPORT

NASA CR-2704

COMBUSTION CONTRIBUTION TO NOISE IN JET ENGINES

E. G. Plett, A. N. Abdelhamid,
D. T. Harrje, and M. Summerfield

Prepared by
PRINCETON UNIVERSITY
Princeton, N. J.
for Langley Research Center

NATIONAL AERONAUTICS AND SPACE ADMINISTRATION • WASHINGTON, D. C. • JULY 1976

1. Report No.	2. Government Accession No.	3. Recipient's Catalog No.
NASA CR-2704		

4. Title and Subtitle	5. Report Date
Combustion Contribution to Noise in Jet Engines	July 1976
	6. Performing Organization Code

7. Author(s)	8. Performing Organization Report No.
E. G. Plett, A. N. Abdelhamid, D. T. Harrje and M. Summerfield	1146
	10. Work Unit No.

9. Performing Organization Name and Address	11. Contract or Grant No.
Princeton University Princeton, NJ	NGR 31-001-241
	13. Type of Report and Period Covered
12. Sponsoring Agency Name and Address	Contractor Report
National Aeronautics & Space Administration Washington, DC 20546	14. Sponsoring Agency Code

15. Supplementary Notes

Langley technical monitor: T. D. Norum

16. Abstract

The relative importance of combustion as a source of noise in a flow regime representative of a subsonic jet engine exhaust was investigated. The combustion noise source characteristics were obtained from pressure and temperature fluctuation measurements in the combustor and exhaust nozzle. The similarity between the fluctuations in this source region and the far field noise were compared, first by examining spectra of each, then by means of cross-correlations and cross-spectral density distributions. In the jet exhaust velocity range between 450 and 660 ft/sec investigated in detail, the frequencies of dominant pressure and temperature fluctuations in the combustor were also the frequencies of the dominant far field noise. The overall noise levels were 14 to 20 dB higher than from a corresponding clean jet in the same velocity range. Thus it seemed clear that the unsteadiness associated with the combustion process was responsible for the dominant noise in the far field. A simple analysis to predict the far field noise due to the internal pressure fluctuations causing exit plane velocity fluctuations produced trends closely resembling the measured results, but under predicted the far field noise over the spectral range examined. The possible reason for the higher far field noise is direct transmission of acoustic waves through the nozzle, which was not accounted for in the prediction scheme.

17. Key Words (Suggested by Author(s))	18. Distribution Statement
Combustion Noise Cross Correlation Noise Spectra Ducted Combustor	Unclassified - Unlimited Subject Category 70

19. Security Classif. (of this report)	20. Security Classif. (of this page)	21. No. of Pages	22. Price*
Unclassified	Unclassified	42	$3.75

* For sale by the National Technical Information Service, Springfield, Virginia 22161

Abstract

The relative importance of combustion as a source of noise in a flow regime representative of a subsonic jet engine exhaust was investigated. Since the research was directed toward understanding noise from a real engine combustor and not the process of combustion per se, the combustion noise source characteristics were obtained from pressure and temperature fluctuation measurements in the combustor and exhaust nozzle. The similarity between the fluctuations in this source region and the far field noise were compared, first by examining spectra of each, then by means of crosscorrelations and cross-spectral density distributions. In the jet exhaust velocity range between 140 and 200 m/sec investigated in detail, the frequencies of dominant pressure and temperature fluctuations in the combustor were also the frequencies of the dominant far field noise. The overall noise levels were 14 to 20 dB higher than from a corresponding clean jet in the same velocity range. Thus it seemed clear that the unsteadiness associated with the combustion process was responsible for the dominant noise in the far field. A simple analysis to predict the far field noise due to the internal pressure fluctuations causing exit plane velocity fluctuations produced trends closely resembling the measured results, but underpredicted the far field noise over the spectral range examined. The possible reason for the higher far field noise is direct transmission of acoustic waves through the nozzle, which was not accounted for in the prediction scheme.

TABLE OF CONTENTS

1. INTRODUCTION

It is well known that unsteady combustion can amplify and generate pressure oscillations in the gaseous medium surrounding the zone of combustion and that these oscillations can be in the audible frequency range. Noise from furnaces and other turbulent flames give evidence to this fact. No general theory or scaling law exists, however, which will allow reliable predictions to be made concerning the importance of combustion as a source of noise in a flow regime such as is found in an aircraft jet engine. Some initial results of a study to provide such information are contained in this report.

Noise generation by open flames has been the subject of several studies during the past twenty years. Giammar and Putnam[1] have presented a review of the experimental work in this area. Several interesting features of combustion noise may be derived from these earlier studies. The characteristic frequencies of combustion noise are found to be considerably lower than for jet noise. Putnam[2] showed, for example, that the noise from his fuel jet with no combustion peaked at around 10 kHz while with the jet burning, the spectrum between 100 and 500 Hz was dominant and at a level of about 20 to 30 dB higher than the peak of the non-burning case. The point of the spectral sound pressure level peak was found to depend upon the type of flame[2] as well as the type of fuel and diameter of the burner[3,4], and the ratio of burner diameter to flow velocity.[5] This Strouhal type scaling suggests that the noise from open turbulent flames is related to the turbulence scale in the flame; the dependence on fuel type suggests some link between the noise generation mechanisms and the chemistry of the reaction. Any theory on combustion noise should therefore contain both of these parameters.

Theoretical work concerning combustion noise has received some attention, but again, mostly related to open flames. Bragg[6] developed a theory on the basis of physical reasoning using the wrinkled laminar flame concept, a concept which is open to question.[7] Kotake and Hatta[5] have also developed a theory for combustion noise. They interpreted observed sound power scaling with flow velocity, U, to the fourth power, to be due to dipole radiation, an interpretation which does not agree with derivations made by Lighthill.[8] Strahle[9] provided a critique of existing theories of combustion noise, and developed two alternative theories of his own. His theories follow more directly from Lighthill's[8] formulation than do the others, and he uses the two existing mechanistic theories for turbulent flames, the wrinkled laminar flame theory and the distributed reaction theory, to derive acoustic efficiencies for flames. In each case he utilizes a proportionality constant which should be near unity in value if the model is accurate. In comparing his theories with

the experiments of Smith and Kilham,[3] he finds the proportionality constants to be 124 and 0.17 respectively for the wrinkled flame and distributed reaction models. It is evident therefore, that further sophistication or more accurate representations of the noise producing mechanisms in flames is clearly needed before accurate predictions of their potential as a noise source can be made.

A general, unified theory of combustion noise has been developed by Chiu and Summerfield.[10] This theory involves a generalized development of the acoustic equations in which temperature variations throughout the source region are allowed, and the temperature in the source region can be different from the temperature in the surrounding medium. The source term is carried through the derivation in a general form so that the solutions can be obtained using any desired model for the unsteady source. Hence, this unified approach allows direct comparisons of flame models, when the unsteady parameters are given. This theory includes contributions from the interaction of fluid turbulence with the unsteady heat release, in addition to the direct contribution from the fluctuating heat release. Strahle's[9] theory includes only the latter effect. Discriminatory diagnostic experiments are needed to determine the relative importance of the various terms in the analytical formulation.

In view of the fact that the predictive accuracy of existing theories of combustion noise have not been proven, it is not surprising that the importance of combustion as a source of noise in jet engines is not well understood. Previous experiments on open flames bear little resemblance to the ducted burner system in an engine, and theories which are derived specifically for, but yet are unproven for the case of open flames, cannot be directly applied to internal combustion systems without verification of their applicability.

If the noise data from a range of aircraft engines is examined,[11] it is apparent that combustion, or some other internal source, is an important source of noise in engines, at least at jet speeds below 350 m/sec , since the overall noise power scaling with jet velocity does not follow the classical U^8 relationship in this range of velocity, as clean laboratory jets may be observed to do. Therefore, it was apparent, at the time that this research was undertaken, that further study of the relative importance of combustion as a source of noise in jet exhausts was needed. This report documents results of a pilot program aimed at this need.

2. PRESENT INVESTIGATIONS

The aim of this investigation was to demonstrate the relative importance of combustion as a source of noise in a flow regime representative of a subsonic jet engine exhaust. The program of research involved measurements of unsteadiness inside a 7.5 cm diameter combustor which exhausted through a 5 cm diameter nozzle, over a velocity range of 150 to 200 m/sec, and measurements of the far field noise due to the combustor/jet combination and correlation of the data. The emphasis in the program was on obtaining experimental evidence of the importance of combustion noise, with analysis being used primarily to correlate the data. Therefore, within the scope of this report, the origin of combustion noise will not be discussed further, but will be accepted as given by measurements obtained inside the combustor. These measurements will be examined with respect to their basic characteristics, such as frequency content and intensity as compared with the far field noise measurements which contain the contribution made by the jet in addition to the noise from the combustor. Analytic expressions are derived and used to predict the far field noise due to the unsteadiness in the combustor. Results of predicted noise levels are compared with measured values.

2.1 Details of Experiment and Data Analysis

In view of the fact that a relatively quick, quantitative demonstration of the relative importance of combustion noise was sought, without an immediate understanding of the detailed mechanisms involved, an experiment was designed for this purpose. A 7.5 cm I.D. combustor was fitted with a 5 cm I.D. nozzle and connected by flexible tubing to metered air and fuel supplies. The combustor assembly was mounted on a pylon 3.7 m above the ground level to minimize ground reflections of the noise which would cause higher readings by far field microphones. Figure 1a shows the firing stand in the open field with microphones stationed at 15° intervals between 15° and 90° to the jet axis, also mounted 3.7 m above the ground, at a distance of 15 m from the combustor exit. Figure 1b is a close-up view of the combustor assembly. Air enters through the flexible hose on the left, flows through an 20 cm I.D. plenum chamber before encountering the flame holder assembly, which is described in more detail below. The hot gases resulting from the combustion process converge and exhaust through the 5 cm I.D. nozzle appearing on the right of Fig. 1b.

Figure 2 shows the details of the combustors used. The upper part of Fig. 2 shows the first design used, designated combustor 'A'. The fuel is injected into a tube which is mounted concentrically within the main combustor. The upstream end of the tube has a constriction which can be adjusted to control the fraction of primary and secondary air.

Near the downstream end of the can is a V-gutter type flame holder which generates turbulence to stabilize the flame. Liquid iso-octane is the fuel used in all the experiments reported. A mixture of hydrogen and air is injected and spark ignited near the flame holder to ignite the iso-octane. The igniter is not on during noise measurements. Pressure transducer ports are located at four stations along the combustor. Only a single transducer, located immediately upstream of the converging nozzle, was used for measurements reported herein.

Combustor 'B' consisted of combustor 'A' with a 20 cm extender inserted between the flame holder and the nozzle, as shown in Fig. 2. The purpose of this modification was to study the effect of combustor length on the noise levels and characteristics.

The lower part of Fig. 2 shows the design of combustor 'C'. Combustor 'C' has a can which is slightly larger in diameter and longer than the tube on 'A', with perforations along the side to allow the air to enter. No primary air enters the upstream end of the can, and the flame is stabilized by a recirculating flow induced at the upstream end of the can.

For equal air and fuel flow rates, combustor 'C' burned slightly more efficiently than 'A' resulting in slightly higher gas temperatures. The acoustic characteristics of the two were also somewhat different, as will be pointed out later. Table 1 summarizes the operating conditions used.

During a given experiment, air and fuel flow rates were measured and the nozzle pressure ratio was measured, all to be used for temperature and efficiency calculations. Noise measurements consisted of simultaneously recording the pressure transducer (Kistler type 601L1) signal along with five microphone (B&K type 4135, 0.635 cm) signals on magnetic tape, using a Honeywell 7600 tape recorder. For signal analysis, the tape was replayed at a later time. One series of experiments involved simultaneous measurement of temperature fluctuations in the nozzle.

Data extracted from the records included sound pressure levels (using a B&K Model 2305 Sound Level Recorder), probability distribution functions, and auto-correlations of the individual signals, as well as crosscorrelations between the pressure fluctuations measured inside the combustor or temperature in the nozzle and the far field noise measurement (all three using a SAICOR Model 43-A, 400 point Correlation and Probability Analyzer). The auto and crosscorrelations were digitized (using a DATACOM Model 8015 A to D converter) and fed into the computer (IBM 360/91), from which power spectral and cross power spectral density distributions were obtained respectively, using a Fast Fourier Transform routine. Some representative data are presented in this report.

The power spectral densities were obtained by Fourier transforming the autocorrelation function. In principle, this yields a power spectral density. Since the "spectral densities" were obtained at 200 discrete frequencies over the interval from 5 to 1000 Hz, each point represents the average power over a 5 Hz bandwidth. As such, they are more correctly termed pressure band levels. These were normalized with respect to the maximum, thus yielding relative levels in dB with respect to the maximum pressure band level of that particular record. The low frequency cut-off of the analysis was at 5 Hz, so no d-c component was observed.

The auto and crosscorrelations were obtained on the SAICOR 43-A correlator. In each case, the correlations were obtained by 1026 x 128 summations, with time increments of 0.50 msec between samples for a total averaging time of just over 1.1 minutes. Although some of the spectra are shown with a range of values greater than 50 dB, the reliable dynamic range was not better than 50 dB.

3. SPECTRUM OF DUCTED COMBUSTION NOISE

Figures 3 through 22 are included here to provide a comprehensive summary of the spectral information obtained from the ducted combustion-noise experiments. Spectral distributions of the chamber pressure fluctuations are shown and compared with the corresponding acoustic spectral distributions at far field points. The spectra shown in this sequence are all obtained by auto or crosscorrelations and subsequent transformation by a Fast Fourier Transform routine, as mentioned in the previous section.

3.1 Chamber Pressure Spectrum

Figure 3 is a plot of the power spectral density distribution of the chamber pressure obtained for operating condition 1, combustor 'A' (see Table 1). Note the spectrum peaks at 5, 50 and 135 Hz, with a sharp drop in power spectral density levels above 135 Hz. There is some evidence of a peak at around 400 Hz, well below the peak at 135 Hz. To get better resolution of the spectrum above 200 Hz, a 250 Hz high pass filter (Ithaco) was used to suppress the low frequency intense fluctuation, allowing the high frequency filtered signal to be amplified without saturating due to the intense low frequency fluctuations. Figure 4 shows the resulting 250 Hz high pass filtered frequency spectrum for the conditions as in Fig. 3. The 400 Hz peak is now more clearly evident, as are peaks around 600 and between 800 and 1000 Hz. It will be noted in the far field acoustic spectral distributions for this case, that these high frequency peaks are much nearer the level of the low frequency peaks than is the case in the power spectral density distribution of the chamber pressure fluctuations.

3.2 Far Field Noise Spectrum - Directionality

Figures 5 through 9 show the acoustic power spectral density distributions for the five microphone locations in the far field, for the same case for which the chamber pressure fluctuations are shown in Figs. 3 and 4. These far field spectral distributions are remarkably similar, indicating that the source of the noise is, at least spectrally, nondirectional. The peak in each of these spectra is at 135 Hz, corresponding to one of the peaks in the chamber pressure spectrum. Below 135 Hz, the far field acoustic spectrum does not resemble the chamber pressure spectrum, while above 135 Hz, its relative peaks do correspond approximately to those in the chamber, but the levels of the higher frequency peaks are much nearer the level of the peak at 135 Hz than in the chamber pressure spectrum. It will be noted in a later approximate analytical development that the high frequency chamber fluctuations may be expected to be more efficient noise generators, due to an effective multiplication by the frequency, as the disturbance passes through the nozzle of the chamber.

3.3 Cross Spectral Density

To verify the relationship between chamber pressure fluctuations and far field acoustic signals, the two were crosscorrelated. Figure 10 shows the resulting crosscorrelation function variation with time, for the case illustrated in Figs. 3 and 8. The dominant tone aspect of the two signals gives rise to the harmonic function like oscillations, while the random noise aspect determines the envelope of the sine function. The time of the peak in the envelope corresponds to the time taken for the sound to travel from the source to the far field receiver, in this case just under 50 msec. Figure 11 shows the cross spectral density distribution obtained via the Fourier transform of Fig. 10. The peaks at 135 Hz and around 400 and 600 Hz verify that the dominant peaks at these frequencies in the acoustic far field signal are due to the fluctuations in the combustor. Here it is clear that the unsteady combustion is the dominant noise source, since the peaks in the acoustic far field spectrum, which have been linked to the combustor pressure fluctuations, are at a much higher level than any other part of the power spectral density distribution. The peaks at around 800 and 1000 Hz in the acoustic spectral distributions are undoubtedly also due to harmonics of the dominant chamber pressure fluctuation, which are lost in noise in Fig. 3, but appear in Fig. 4 when the high frequency range is selectively amplified.

3.4 Spectrum Dependence on Operating Conditions

For a comparison of the spectral content of noise from this combustor with a given geometry and flame holder, we compare Figs. 8, 12, 13 and 14. Figures 8 and 13 are for an air/fuel ratio of 40 at two flow rates. The spectral content of these two cases is almost identical, except that the lower flow rate case, Fig. 13, has relatively more intense noise below 50 Hz. This ultra-low frequency noise is associated with unsteady flame motion in the combustor, which was operating less smoothly for conditions A-2, 3 and 4 than for condition A-1 (Table 1).

Figure 12 is for the same, approximate overall flow rate as Fig. 8, but a leaner mixture is used which gives rise to a more uniform level for all the spectrum peaks between 40 Hz and 830 Hz. Figure 13 is for the same air/fuel ratio as Fig. 12, but with a lower flow rate. Again in this case, the lower flow rate leads to more intense, ultra-low frequency oscillations.

It would appear, from the four figures compared here, that there may be an ultimate operating condition for a given combustor and flame holder geometry which would minimize the level of fluctuation. It is not clear from these figures alone, what that optimum condition might be, but the variation of spectral content with flow rate and air/fuel ratio suggests that some such condition exists. More detailed study is required in this area.

3.5 Spectrum Dependence on Duct Length

Figure 15 shows the power spectral density distribution obtained with combustor 'B', which is identical with combustor 'A' except that 20 cm length of ducting has been added, as shown in Fig. 2. The effect of this additional length is to give the fuel more time to complete combustion, and it also provides a longer resonant cavity for longitudinal flow oscillations. The spectrum is most directly affected by this latter effect. The longer cavity results in slightly lower frequencies for the main peaks, as illustrated by comparison of Figs. 15 and 8. Even this difference is very slight at this operating condition.

It will be noted later that the overall noise levels generated by combustors 'A' and 'B' were very nearly the same, with 'B' giving slightly less noise in general. This slight difference may be partially due to the lower frequencies in 'B'; low frequency oscillations are generally less efficient noise sources than higher frequency oscillations.

3.6 Spectrum Dependence on Flame Holder Configuration

Detailed studies were carried out with combustor 'C', which is also depicted in Fig. 2. The differences between 'A' and 'C' were described in Section 2 of this report.

Figure 16 shows the power spectral density of the combustion chamber pressure oscillations for operating condition 2, combustor 'C' (the flame blew out with condition 1). Several differences may be noted from earlier spectral distributions shown, and several similarities are evident. As with 'A' and 'B', there is one dominant spectral peak, with less intense peaks at other frequencies. The shape of the spectral peak with 'C' is less pointed than with the others, indicating narrow band noise, as opposed to almost a tone-like quality in 'A' and 'B' at the main peak. The frequency of the main peak is slightly higher with 'C', possibly attributable to the higher temperature attained with this combustor (Table 1) resulting in a higher effective sound speed and related higher frequency for the corresponding resonance length.

Figures 17, 18 and 19 show far field noise spectral distributions for the three operating conditions of combustor 'C'. Again, as with 'A', the frequencies above the main peak are higher, relative to the main peak, than in the combustion chamber and the lower frequencies are less evident. Again there are some differences with operating conditions, and as with combustor 'A', these differences are more in relative level of spectral peaks than in frequency of the peaks.

The autocorrelations of the chamber pressure fluctuations and the far field acoustic signals are also of interest to compare for the cases being compared. Included here as Figs. 20 and 21 are such typical records for the chamber pressure fluctuation of combustors 'A' and 'C' respectively. The power spectral density obtained from the autocorrelation shown as Fig. 20 is shown in Fig. 3, and similarly Figs. 21 and 16 correspond. The dominant frequencies can be observed in the autocorrelations.

The crosscorrelation between chamber pressure fluctuations and far field acoustic signals was discussed earlier for combustor 'A' (Figs. 10 and 11). Similar crosscorrelations were obtained for combustors 'B' and 'C'. Figures 22 and 23 show the crosscorrelation and cross spectral density distribution for operating condition 2, combustor 'C'. As the autocorrelations differ for these two combustors, Figs. 20 and 21, so the crosscorrelations differ, Figs. 10 and 22. Similarly, the cross spectral density distributions obtained from the respective crosscorrelations show the dominant frequencies observed in the individual spectra (compare Fig. 23 with 16 and 17 and Fig. 11 with 3 and 8).

Therefore, it may be noted that the two geometries of flame holders have resulted in different shapes for the power spectral density distributions, and have generated slightly different peaks in the spectra, but the harmonic type oscillations appear for both cases.

3.7 Spectrum with Air Flow, No Combustion, Compared with Spectrum with Combustion.

Figure 24 shows the power spectral density distribution obtained with only air flow, no combustion, as observed in the far field. The dominant spectral peaks observed for cases with combustion, in this frequency range are absent. The dominant unsteadiness in this range to 1000 Hz is at very low frequencies. Therefore, the very low frequency noise observed in the spectra with combustion may be attributable to flow unsteadiness entering the combustor. Very clearly, though, the observed spectral peaks at around 200, 400, 600 Hz etc., as previously discussed, are due to the unsteadiness introduced by the combustion process.

Figure 25 is for a slightly different case. Here, the combustor can, 'C', was allowed to protrude out of the end of the duct, so that about two-thirds of the can was visible beyond the duct end. Figure 25 shows the power spectral density distribution for the case with only air flowing over this modified combustor arrangement. The range of highest spectral intensity is between 2000 and 2500 Hz, and the ultra low frequency peak is again visible. The peaks so commonly seen between 150 and 1000 Hz for cases with combustion are not important in this case.

Figure 26 shows the power spectral density distribution for the same case as Fig. 25, but with combustion in this case. The striking difference between Figs. 25 and 26 is the addition of the intense noise in the spectral range below 1000 Hz, with spectral peaks at around 200, 400, 600, 800 and 1000 Hz. Clearly, this additional noise content is directly attributable to the nonsteady combustion process. It is interesting that approximately the same peak frequencies are observed with this partially confined case as with the cases discussed earlier for which the combustor can was well inside the duct.

More details regarding the effect of the confining duct are given in reference 12.

4. RELATIVE IMPORTANCE OF COMBUSTION AND JET NOISE

4.1 Overall Sound Pressures in Far Field

In evaluating the relative importance of combustion as a source of noise, it is necessary to make quantitative comparisons.

Figures 27 through 30 give quantitative comparisons of the noise emitted by the three combustor configurations at each of four operating conditions, all far field measurements being taken at a distance of 15 m. Figure 27 compares the noise output of combustors 'A' and 'B', at operating condition 1 (Table 1). As may be observed, there is little difference between them. Since the rms roughness inside the two combustors is about the same, the slight difference in overall sound pressure level in the far field may simply be due to the lower characteristic frequencies in 'B' which radiate sound less efficiently than higher frequencies.

Figure 28 similarly compares the noise output of the three combustors at operating condition 2. 'A' is again slightly noisier than 'B',and 'C' is slightly noisier than 'A'. The dominant frequency of 'C' is again higher than that of either 'A' or 'B', but the internal roughness of 'C' is slightly less than that of 'A' or 'B'. Figure 29 offers the same comparison at operating condition 3. At this condition, combustor 'C' is much noisier than 'A' or 'B', which are again essentially equal. In Fig. 30, for operating condition 4, combustors 'A' and 'B' are again essentially equally noisy, while 'C' produces about 5 dB higher noise intensities than the other two. In Fig. 30, a noise curve for ambient temperature air flow through combustor 'C', at about 0.25 Mach number, i.e., the same as the hot flow Mach number, is shown. The difference in noise level for the case with combustion compared with the case with no combustion, at the same Mach number, is about 14 dB. The noise from this cold flow is undoubtedly higher than for a clean jet, due to the flow obstructions inside the duct but still 14 dB lower than the equivalent case with combustion. The dominant frequency for this cold flow was in the vicinity of 4000 Hz while at the same Mach number, in combustor 'C', the hot flow had a dominant frequency of 205 Hz.

4.2 Normalized Crosscorrelations

Direct, real time crosscorrelations between pressure fluctuations inside the combustor and the far field sound were made. Figures 10 and 22 are examples of the traces obtained for these crosscorrelations.

It is well known that two random signals which have frequency and phase relations in common will produce a finite crosscorrelation while two unrelated random signals will

produce a crosscorrelation of zero value. The degree of "sameness" between the two signals crosscorrelated determines the magnitude of their crosscorrelation. If there is a one to one correspondence between the two signals, their normalized crosscorrelation will be unity, where the normalized crosscorrealtion is given by

$$\rho_{ab} = \frac{1}{T} \int_0^T \frac{S_a(t) \cdot S_b(t+\tau)\, d\tau}{\sqrt{|S_a|^2} \cdot \sqrt{|S_b|^2}} \qquad (1)$$

The time delay "c" in the integrand is to allow the wave form passing "b" to reach "a". In our case, it is to account for the time taken for the sound generated in the combustor at time 't' to propagate to the far field where it arrives at time 't + τ', where $\tau = r/c$, the distance travelled divided by the sound speed.

Figure 31 shows the values of the normalized cross-correlations obtained for several combustor operating conditions, when the fluctuating combustor pressure was cross-correlated with the far field pressure. From this plot it is evident that there is considerable frequency and phase similarity between these two quantities, with combustor 'C' exhibiting a stronger similarity.

4.3 Scaling of Sound Power

Figure 32 shows the overall sound power obtained from measurements on combustors 'A' and 'C' compared with the sound power from a clean jet of equal size, plotted with Mach number on the abscissa. Comparison on the basis of equal Mach number implies equal thrust. On this basis, if it was possible, a clean cold jet could generate substantially more thrust with much less noise. Or, stating the comparison another way, for a given jet Mach number, the flow originating in the combustion chamber generates several orders of magnitude more noise than a flow exhausting from a smooth duct with no combustion. The hexagonal point in the center of Fig. 32 reminds one that the obstructions, such as the burner can and struts inside the combustor, account for some of the excess noise even in the absence of combustion. Nevertheless, the case with combustion is still 14 to 20 dB noisier than the cold flow case in the same combustor, at the same Mach number.

Figure 33 shows the same comparison on the basis of jet velocity. On this basis there is less difference between the clean cold jet and the jet originating inside a combustion chamber. The noise from the combustors is now only 10 to 20 dB in excess of the jet noise.

These two figures (32 and 33) very emphatically demonstrate that combustion upstream of a jet nozzle will increase the noise power (for the same jet velocity) by a factor of between 10 and 100, depending on the roughness level inside the combustor. An analytical relationship to link the roughness inside the combustor to the noise level produced outside is needed. Some attempts have been made to produce such a relationship. Section 5 of this report outlines the approach taken to date.

4.4 Smoothed Flow

An attempt to reduce the external noise contribution from the rough combustion was made by placing a honeycomb type flow straightener in the duct upstream of the nozzle. The straightening section was 3.75 cm long and consisted of 22 passages of 1.25 cm diameter and 10 passages of 0.47 cm diameter as well as 2 of 0.78 cm diameter. The smaller holes were added merely to provide as much flow area as possible across the 7.5 cm diameter duct cross section.

The flow straightener did not appreciably change the level of roughness inside the combustor. The far field noise was changed somewhat, however, as may be seen from Fig. 34. The point at 30° from the jet axis was unchanged while the 60° point was about 3 dB lower with the straightener than without it for conditions corresponding to combustor condition C-2 (Table 1), and the 90° point was suppressed about 2 dB. The data used here for the case without the flow straightener do not correspond exactly to those plotted on Fig. 28, since they were conducted with a slightly different nozzle contour. The two cases compared in Fig. 34 were the same in every way, except for the flow straightener in one case.

Several different cases were examined with this flow straightener, and the noise reductions were approximately the same for each case.

5. ANALYTICAL PREDICTION OF NOISE FROM COMBUSTOR PRESSURE FLUCTUATIONS

5.1 Overall Procedure

It would be of considerable interest to be able to simply monitor the pressure fluctuations inside a combustion chamber and by some analytical procedure predict reliably what the noise level outside would be. It now appears, after closer examination, that we need to know both the temperature and pressure fluctuations in the combustor, but for a beginning we tried using only the pressure.

Two steps were envisioned in this prediction scheme. Since the sound generated by internal sources is best evaluated in terms of a surface integral of the appropriate quantities across the exit plane of the exhaust nozzle, the first step was to predict what these terms would be at the exit plane, using measurements inside the combustor, and the second step would be to calculate the noise generated at the exit plane. From Curle's[13] general solution, we know that the overall noise generated by a jet is given by

$$p' = \frac{1}{4\pi c^2} \frac{x_i x_j}{|\bar{x}_i|^3} \frac{\partial^2}{\partial t^2} \int_{V_0} [T_{ij}] dV_0$$

$$- \frac{1}{4\pi c} \frac{x_i}{|x_i|^2} \frac{\partial}{\partial t} \oint_{S_0} [\rho v_i v_j + p_{ij}] \cdot dS_0$$

$$+ \frac{1}{4\pi} \frac{1}{|\bar{x}|} \frac{\partial}{\partial t} \oint_{S_0} [\rho v] \cdot dS_0 \qquad (2)$$

Here the first term represents the jet noise sources and the other two terms are integrals over all adjacent bounding surfaces which might contribute to the noise. The jet exit plane is clearly one such surface. The third term in Eq. (2), is believed, in the present case, to be the dominant one. Therefore, attempts have been made to evaluate the noise due to mass flow fluctuations at the exit plane caused by unsteadiness inside the combustor.

5.2 Ultra Low Frequency, Quasi-Static Approximation: Method I

Assuming a constant density, inviscid flow between the chamber and nozzle exit, Bernouli's equation, applicable along stream lines, may be applied in the form

$$\rho\frac{\partial u}{\partial t} + \rho\nabla\frac{1}{2}u^2 = -\nabla p \tag{3}$$

For this first order solution, the integral along the stream lines will neglect the first term in Eq. (3) resulting in Eq. (4).

$$\frac{1}{2}\rho u_2^2 + p_2 = \frac{1}{2}\rho u_1^2 + p_1 \tag{4}$$

where subscript (1) will denote conditions in the combustor and (2) will denote exit plane conditions. Then assuming a perturbation type solution with $u_1 = u_{01}$, $u_2 = u_{02} + u_2'$, $p_2 = p_{02}$ and $p_1 = p_{01} + p_1'$, Eq. (4) may be reduced to a quasi-steady and a perturbed solution. The perturbed form may be written as

$$u_2' = p_1'/\rho_0 u_{02} \tag{5}$$

Using Eq. (5), the exit plane velocity fluctuations may now be evaluated from chamber pressure fluctuations. If the exit plane is now considered to be a simple monopole, the noise in the far field can be shown to be[14]

$$p_f = \frac{\rho_0 u_2' \omega a^2}{r_f\sqrt{2}} \tag{6}$$

where $\omega = 2\pi f$, is the angular velocity of the fluctuation, a is the nozzle radius and r is the distance to the far field point. When Eq. (6) is combined with Eq. (5), the far field noise is calculable in terms of the chamber pressure fluctuation; i.e.,

$$p_f = \frac{p_1'}{\sqrt{2}}\left(\frac{\omega a}{u_{02}}\right)\frac{a}{r_f} \tag{7}$$

One further factor should be included. Equation (6) is derived for a source in a constant temperature region all the way to the measuring point. If a temperature (acoustic impedance) change occurs between these points, the acoustic energy transmitted will be equal to the incident energy times a transmission coefficient, where the transmission coefficient is evaluated based on the impedance change.[15] For this case, assuming ideal gas behavior, the pressure

fluctuation will be enhanced by the temperature drop. The modified expression is given by Eq. (8).

$$p_f = \frac{p'_i}{\sqrt{2}}\left(\frac{\omega a}{u_{02}}\right)\left(\frac{a}{r}\right)\left(\frac{2(c_h/c_f)}{(c_h/c_f) + 1)}\right) \tag{8}$$

This additional factor accounts for an increase of about 2.4 dB in the calculated levels.

5.3 Higher Frequency Effects: Method II

The ultra low frequency approximation neglected pressure fluctuations at the subsonic nozzle exit; the quasi-static approximation neglected the integral of the first term of Eq. (3) through the converging nozzle. If, instead of neglecting these two effects, we account for them in an approximate way, the effects of higher frequency components in the flow fluctuation become more apparent. The open end pressure fluctuation is accounted for in terms of the product of a complex impedance, $z = z_r + iz_i$, and the velocity fluctuation. The streamwise integral of the velocity time derivative results in a term containing a length, ℓ, and an angular velocity ω. If, in addition, the finite size of the duct upstream of the nozzle is accounted for, the expression for the velocity fluctuation at the exit plane may be written in complex form as

$$u'_2 = \frac{p'_i\left[\left(1 - \left(\frac{r_2}{r_1}\right)^4 + \frac{z_r}{\rho_0 u_{02}}\right) - i\left(\frac{z_i}{\rho_0 u_{02}} + \frac{r_2}{r_1}\frac{\ell\omega}{u_{02}}\right)\right]}{\rho_0 u_{02}\left|\left(1 - (r_2/r_1)^4 + \frac{z_r}{\rho_0 u_{02}}\right)^2 + \left(\frac{z_i}{\rho_0 u_{02}} + \frac{r_2\ell\omega}{r_1 u_{02}}\right)^2\right|} \tag{9}$$

In the case of a conically tapered nozzle and an incompressible relation for the velocity in the nozzle, the length parameter, ℓ, corresponds to the length of the taper in the nozzle.

If the nozzle exit plane is assumed to behave as a simple acoustic source with velocity fluctuations as given by Eq. (9), the far field sound pressure level due to this source is given as

$$p_f = \frac{a}{r_f}(z_r + iz_i)u'_2$$

or

$$p_f = \frac{\left(\frac{\omega a}{u_{02}}\right)\left(\frac{a}{r_f}\right)\left\{\frac{\omega a}{4c_h}\left[1 - \left(\frac{r_2}{r_1}\right)^4 + \frac{\omega^2 a^2}{4u_{02}c_h}\right] + 0.6\left[\frac{0.6\omega a}{u_{02}} + \frac{r_2}{r_1}\frac{\ell\omega}{u_{02}}\right]\right\}p_i'}{\left|\left[1 - \left(\frac{r_2}{r_1}\right)^4 + \frac{\omega^2 a^2}{4u_{02}c_h}\right]^2 + \left[\frac{0.6\omega a}{u_{02}} + \frac{r_2\ell\omega}{r_1 u_{02}}\right]^2\right|} \qquad (10)$$

when $z = \rho_0 c_h\left[\frac{\omega^2 a^2}{4c_h^2} + i0.6\frac{\omega a}{c_h}\right]$ is assumed.

Finally, the propagation of the emitted sound through the jet boundary which constitutes a change of acoustic impedance, results in an intensification of the sound by a factor $2(c_h/c_f)/((c_h/c_f) + 1)$, where c_h is the sound speed in the hot jet exit plane, c_f is the sound speed surrounding the jet. As discussed in connection with Eq. (8) this intensification adds about 2.4 dB to the far field sound pressure levels, over that calculated by Eq. (10).

The usefulness of Eqs. (7) and (10), or their modified form including the impedance change intensification, were tested in connection with experimental results. These comparisons are discussed in the next section.

5.4 Comparison of Analytical Predictions with Experimental Results

The first comparison to be made is the overall observed sound pressure level in the far field with that predicted by the two analytical expressions. From the many spectra shown in connection with Section 3 of this report, it is apparent that several spectral peaks stand out in the chamber pressure spectrum, and in the far field spectrum. If, for the purpose of calculations, we assume that all the acoustic energy is concentrated in the dominant spectral peak, a simple one step calculation will yield the predicted far field sound pressure level from the level of internal pressure fluctuations using the equations given in Sections 5.2 and 5.3. Figures 35, 36 and 37 show the resulting points compared with measured values for the three combustors studied (if a single source filling the exit plane is assumed).

It is clear from these three figures that calculation method I gives more accurate results for cases A-2, A-4, B-2 and B-4, all of which had dominant spectral peaks at very low frequencies, between 35 and 50 Hz. For the other cases, for which the dominant spectral peak was between 125 and 210 Hz,

the first method predicted higher noise levels than were measured in the far field.

Predictions by method II were far too low for the very low frequency cases, and still low but closer to measured far field results for the cases with dominant spectral peaks at higher frequencies.

It appears from these comparisons that using a single spectral peak to represent the overall noise is not adequate, at least with this set of cases examined by the methods described. It may also be inferred that the impedance functions used for calculating pressure-velocity relations at the exit plane were not exactly applicable. Method I assumed the impedance to be effectively zero for calculating the velocity fluctuation at the exit plane, and used a spherical source impedance at the exit plane to calculate the far field noise. Method II assumed, for both parts of the calculation, that the impedance was like that of an unflanged pipe end. Perhaps an impedance function measured for these flow conditions would give better results in computations.

A further comparison was made for one case using 1/3 octave pressure band levels to predict corresponding levels in the far field at each frequency. Figure 38 shows the combustor pressure spectrum used as input to these calculations and Fig. 39 shows the predicted results from each of the two methods described. Although Method I overpredicted the far field levels for this case when a single frequency representation was used, Fig. 37, here it underpredicts at all frequency bands. The deviation at very low frequencies may be due, largely, to background noise in the far field, which did not have its origin inside the combustor. Over the remainder of the spectrum, the Method I prediction scheme underestimated the far field noise by 7 to 8 dB. Predictions by Method II were 6 to 10 dB below those of Method I at frequencies above 180 Hz, but fell away more sharply below this frequency range.

It appears that a better method of predicting far field noise levels due to internal pressure fluctuations is needed. One ingredient for such a better method would be an exit plane impedance function which is applicable for this geometry and these flow conditions. No such function is currently available. The method reported herein is over simplified. A more complete analysis is needed.

6. TEMPERATURE FLUCTUATION EFFECTS

6.1 Measurement of Temperature Fluctuations

To obtain meaningful measurements of temperature fluctuations in the combustion gases is considerably more difficult than to obtain pressure fluctuations. The basic reason for the greater difficulty is the fact that the temperature probe must be immersed in the hot, reacting flow, while the pressure probe can be mounted on the wall where it can be cooled and insulated from the flow.

A hot wire anemometer system in conjunction with a 0.025 mm diameter platinum wire was used to make the measurements reported herein. The velocity sensitivity of the probe was minimized by maintaining a low probe current (1.5 ma) which kept the wire just above the ambient temperature. Therefore, as the ambient temperature fluctuates, the wire temperature follows, and the anemometer circuit gives an output proportional to wire resistance which is temperature dependent.

Difficulties were encountered due to the high temperature reactive flow. A metal's strength is generally reduced as its temperature is raised, so although the wire may not melt, it is more easily broken at elevated temperatures. In addition, certain metals such as tungsten catalyze recombination reactions which can result in large errors as the probe temperature is raised due to additional energy deposition at its surface. Thus, early attempts with tungsten wires yielded unreliable data, and platinum was adopted, in spite of its lower strength.

The maximum temperature recommended for this probe was about 1100°K, which was considerably lower than the mean temperature in previous runs, as can be seen from Table 1. Therefore, an even leaner mixture had to be used in order to bring the temperature down. An air/fuel ratio of 70 was adopted for this purpose, which should give a mean temperature of about 860°K, in the nozzle, but since hot spots can occur in such a system, this seemed a safe condition at which to operate.

The probe used for the temperature measurements was a Thermo Systems Model 1226 High Temperature probe with a 0.025 mm diameter platinum wire. It was inserted through the nozzle wall so that the wire was held at the duct centerline in the same axial plane as the nozzle pressure transducer, about 3.1 cm upstream of the nozzle exit. The 5 cm diameter nozzle was used in these experiments.

6.2 Spectrum and Level of Temperature Fluctuations

Since the operating condition chosen was different from any previously discussed in this report, the spectra of far field noise and internal pressure fluctuations are also different. The comparisons which follow will therefore show

the corresponding spectra of far field noise and internal pressure fluctuations for this condition as well as the measured temperature fluctuation spectrum.

Figure 40 shows the power spectral density of the nozzle temperature fluctuations. A very low frequency fluctuation is dominant with the first peak at 5 Hz, which is the lower limit of the spectral analysis. Relative peaks next occur at 125 and 165 Hz, with a subsequent intensity decrease to the instrumentation noise levels. Figure 41 shows the corresponding far field noise spectrum which exhibits the 165 Hz peak, but does not exhibit the strong low frequency content seen in the temperature spectrum; instead it shows approximate higher harmonics of the 165 Hz peak. The power spectrum of the temperature signal with low frequencies suppressed by a 100 Hz high pass filter is shown in Fig. 42. The 165 Hz peak is now dominant, with another relative peak at 330 Hz. At frequencies above that peak, the noise level of the electronics is dominant over any temperature signal. This may be expected, since the thermal time constant of the wire under these operating conditions is about 2.5 msec, having the effect of filtering out frequencies above about 400 Hz. Either the circuitry does not compensate for this decrease of response with increased frequency, or there is negligible fluctuation in temperature above this frequency. Further experiments with smaller wires are required to explore this further.

The absolute, rms level of temperature fluctuation in the 125 - 160 Hz, 1/3 octave band was measured to be about 7 Kelvin degrees, or a little more than 1% of the mean temperature. The overall rms temperature fluctuation in the frequency range from 22 Hz to 22 kHz was measured to be about 20% of the mean temperature, with peak to peak variation considerably higher. The results presented here do not show a strong relationship between this temperature unsteadiness and noise possibly due to crude measurements. Further studies with more refined instrumentation are required to establish its relative importance.

6.3 Crosscorrelations of Temperature Fluctuations and Far Field Sound

Figure 43 shows the cross spectral density of the nozzle temperature fluctuation and the far field sound, for no low frequency elimination of either signal. The dominant low frequencies noted in the individual frequency spectra are evident in this cross spectrum. The normalized crosscorrelation coefficient was found to be 0.05 for this case.

It would seem, on comparing Figs. 40 and 41, that the very low frequency (below 100 Hz) temperature fluctuations do not

substantially contribute to the far field noise. A second crosscorrelation between these same two signals was obtained, this time with a 100 Hz highpass filter cutting out the low frequency content of each signal. The resulting cross spectral density is shown in Fig. 44. The normalized crosscorrelation coefficient in this case is 0.276, or more than five times as large as for the unfiltered signal. This higher correlation after filtering out the intense fluctuations at ultra low frequencies illustrates that a simple overall crosscorrelation coefficient is not sufficient information to determine the percentage of far field noise which originated at the source being probed.

6.4 Summary of Temperature Fluctuation Results

We have obtained data on the temperature fluctuations in the flow exhausting from a combustion region. The spectral densities of the temperature and noise signals and their cross spectral densities indicate that there is considerable similarity between them, at least in the frequency range between 100 and 200 Hz, where the temperature probe had adequate response. The ultra low frequency temperature fluctuations were not significant contributors to the far field noise as evidenced by the higher normalized crosscorrelation obtained when this ultra low frequency content was filtered out.

A more complete study of the relationship between temperature fluctuations and noise is needed. In addition, more refined instruments and methods to measure these temperature fluctuations over a broader frequency range is needed before their full significance as noise sources can be evaluated.

7. SUMMARY AND CONCLUSIONS

This program of research was intended to provide information regarding the relative importance of combustion as a source of noise in jet engines. To accomplish this, experiments were performed with a ducted combustor which exhausted through a 5 cm diameter nozzle at speeds in the range of 140 to 200 m/sec at temperatures representative of jet engine exhaust temperatures. To evaluate the contribution from the nonsteady combustion in this configuration, it was necessary to identify which part of the far field noise was due to combustion. This was done by examining the spectral content of the chamber pressure and temperature fluctuations and comparing with the spectrum of the far field noise. Crosscorrelations were used to obtain cross spectral densities. In addition, the sound power for this jet flow with rough upstream internal combustion was compared with the sound power of a similar jet flow without upstream internal combustion. The case with rough upstream combustion was found to be 14 to 20 dB noisier for corresponding flow velocities.

The power spectral density distribution of combustion generated noise was observed to be dominantly in the low frequency range, with several dominant spectral peaks below 1000 Hz, corresponding to the 1/4 wave tube cavity excitation and several higher harmonics. The same narrow band spectral peaks appearing inside the combustion chamber were observed in the far field noise spectrum. Direct crosscorrelations, and associated cross spectral densities verified that a large part of the noise observed in the far field originated inside the combustor.

Comparison of noise levels from the combustor exhaust with clean jet noise levels, either on the basis of jet velocity or jet Mach number, show the combustor exhaust to be much noisier. The noise level of the combustor exhaust depends upon the combustion roughness and frequency of oscillations; these vary with fuel/air ratio, combustor geometry and overall mass flow through the combustor. A honeycomb type flow straightener just upstream of the nozzle was observed to reduce the far field noise by about 3 dB at 60° to the jet axis, with somewhat smaller reductions at 90° and near the jet axis.

Attempts were made to analytically predict the far field noise due to velocity fluctuations at the nozzle exit which were driven by internal pressure fluctuations. The predicted levels gave trends which closely resembled the far field signature, but were slightly lower than observed levels. Possible reasons for the discrepancy were the direct transmission of acoustic waves through the nozzle, which were not accounted for in this simple analysis, or ground reflections which produce higher noise levels in experiments than would

be obtained by direct radiation only. Both of these possibilities must be further investigated in order to develop a reliable method of predicting far field noise due to internal, rough combustion. The analysis used here is perhaps oversimplified and a more complete analysis is needed.

Measurements were made to obtain better information regarding the role of temperature fluctuations as a noise source in a hot combustor exhaust. The results showed some direct correspondence between the temperature spectrum and the far field noise spectrum. No theoretical analysis was conducted, within the scope of this pilot program, to further elucidate the possible relationship between temperature fluctuations and noise. Such an analysis and more refined experiments in support of the analysis are recommended as an important further advancement of the research on combustion noise and its relative importance in jet engines.

1. Giammar, R. D. and Putnam, A. A., "Combustion Roar of Turbulent Diffusion Flames," J. of Eng. for Power, Vol. 92, Ser. A, pp. 157-65 (1970).

2. Putnam, A. A., "Flame Noise From the Combustion Zone Formed by Two Axially Impinging Fuel Jets," Univ. of Sheffield Fuel Society Journal, Vol. 19, pp. 8-21, (1968).

3. Smith, T. J. B., and Kilham, J. K., "Noise Generation by Open Turbulent Flames," J. Acous. Soc. of America, Vol. 35, pp. 715-724, (1963).

4. Knott, P. R., "Noise Generated by Turbulent Non-Premixed Flames," AIAA Paper No. 71-732, June 1971.

5. Kotake, S., and Hatta, K., "On the Noise of Diffusion Flames," Bull. JSME, Vol. 8, No. 30 pp. 211-219, (1965).

6. Bragg, S. L., "Combustion Noise," J. of the Inst. of Fuel, 36, p. 12-16, (1963).

7. Summerfield, M., Reiter, S. H., Kebely, V., and Mascolo, R. W., "The Structure and Propagation Mechanism of Turbulent Flames in High Speed Flow," Jet Prop., Vol. 25, No. 8, pp. 377-384 (1955).

8. Lighthill, M. J., "On Sound Generated Aerodynamically, I. General Theory," Proc. Roy. Soc., A211, pp. 564-587, (1952).

9. Strahle, W. C., "On Combustion Generated Noise," J. Fluid Mech., Vol. 29, part 2, pp. 399-414 (1971).

10. Chiu, H. H. and Summerfield, M., "Theory of Combustion Noise," 4th International Colloquium on Gasdynamics of Explosions and Reactive Systems, San Diego, (1973).

11. Bushell, K. W., "A Survey of Low Velocity and Coaxial Jet Noise with Application to Prediction," J. Sound and Vibration, 17(2), pp. 271-282, (1971).

12. Chiu, H. H., Plett, E. G., and Summerfield, M., "Noise Generation by Ducted Combustion Systems," AIAA Paper 73-1024, Oct. 1973.

13. Curle, N., "The Influence of Solid Boundaries Upon Aerodynamic Sound," Proc. Roy. Soc., Vol. 231A, pp. 505-514 (1955).

14. Plett, E. G. and Summerfield, M., "Estimates of the Contribution to Jet Engine Exhaust Noise Made by Internal Sources," Paper XX6, presented at the 84th Meeting of the Acoustical Society of America, Miami Beach, 28 Nov. - 1 Dec. 1972.

15. Morse, P. M. and Ingard, K. U., Theoretical Acoustics, McGraw Hill, N.Y., 1968, p. 471 ff. and p. 711.

Table 1

Combustor Operating Conditions

Combustor-Condition	A/F Ratio	Jet Mach Number	Exhaust Gas Total Temp. (°K)	Combustion Efficiency (%)	Jet Vel. (m/sec)	Internal Overall RMS Roughness (dB)
A - 1	40	0.288	1200.	96.9	200.	158.
A - 2	50	0.290	1005.	90.9	185.	159.
A - 3	40	0.220	1155.	90.28	160.	157.
A - 4	50	0.243	970.	85.18	150.	158.
B - 1	40	0.288	6970.	95.76	198.	158.
B - 2	50	0.289	996.	89.5	182.	159.
B - 3	40	0.238	1162.	90.05	162.	157.
B - 4	50	0.247	917.	77.89	143.	158.
C - 1	40	Unstable				
C - 2	50	0.3037	1100.	100.+	201.	156.
C - 3	40	0.2407	1222.	97.2	168.	160.
C - 4	50	0.258	1087.	100.+	170.	155.

+The temperature was calculated from gas dynamic relations using measured mass flow and pressure drop through the nozzle, assuming a 100% efficient nozzle. The temperature computed on this basis may be expected to be higher than the actual temperature, hence resulting in a computed combustion efficiency which is too high.

FIGURE 1a Combustor/jet source on 3.7 m high pylon, showing 3.7 m high microphone mounts in one quadrant at 15 m radius.

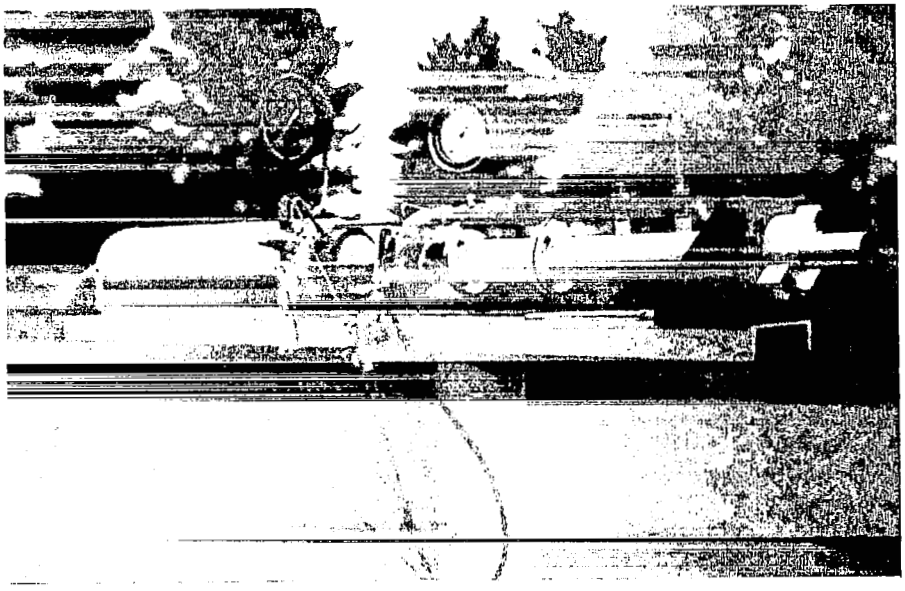

FIGURE 1b Closeup view of combustor in configuration 'B' showing 5 cm nozzle, probe ports and plenum.

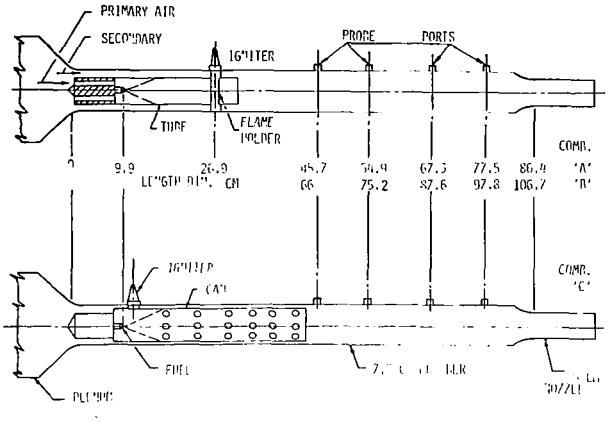

Fig. 2 Schematic to approximate scale of three combustor configurations used. Combustors 'A' and 'B' are identical except that 'B' is 20 cm longer than 'A'; combustor 'C' has no primary air, but secondary air enters through perforations in the can.

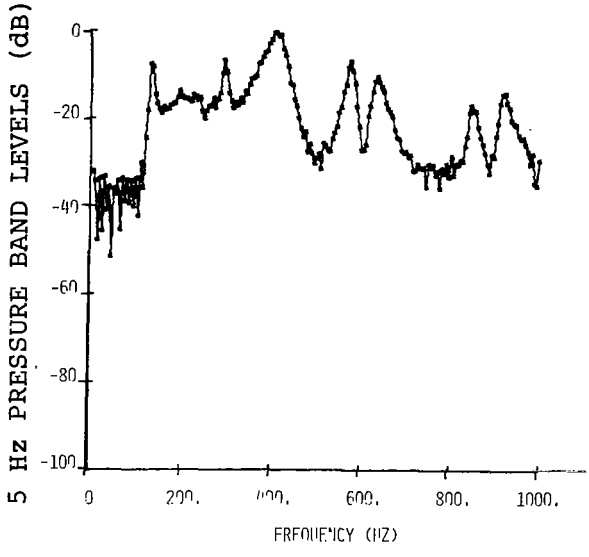

Fig. 4 Power spectral density distribution, with low frequency suppressed by a 250 Hz highpass filter, for combustor 'A', air/fuel ratio = 40, M_j = 0.29.

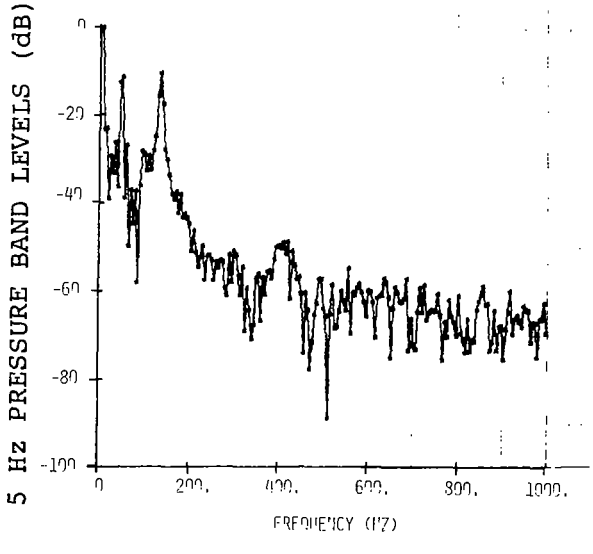

Fig. 3 Power spectral density distribution of chamber pressure, combustor 'A' air/fuel ratio = 40, M_j = 0.29

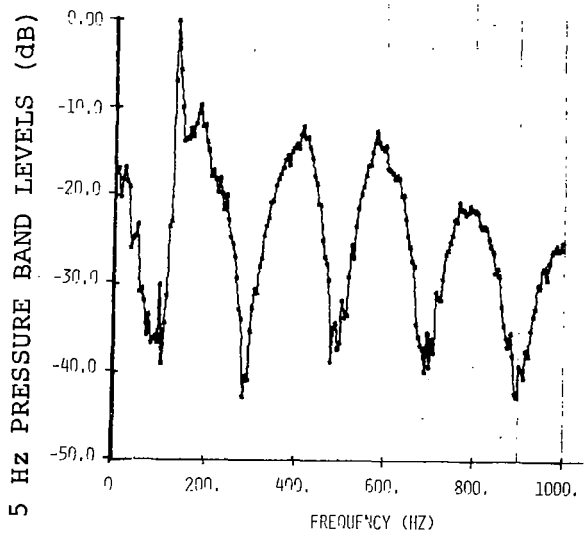

Fig. 5 Power spectral density of far field sound for the same condition shown in Figs. 3 and 4. This plot is from the microphone at 15° to the jet axis, 15 m from the combustor exit.

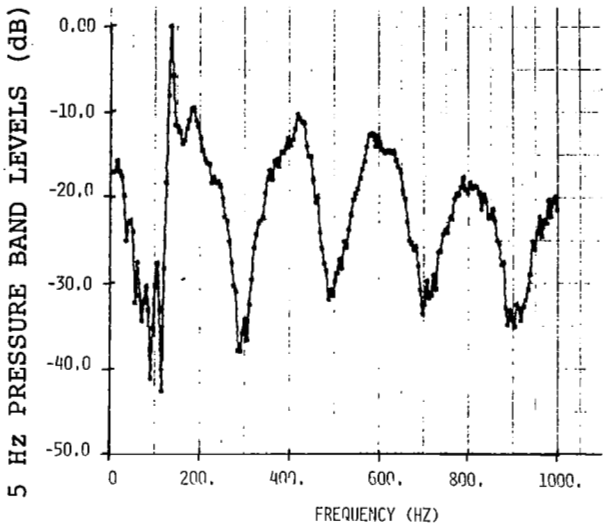

Fig. 6 Same condition as Figs. 3-5, far field spectrum at 30° to jet axis.

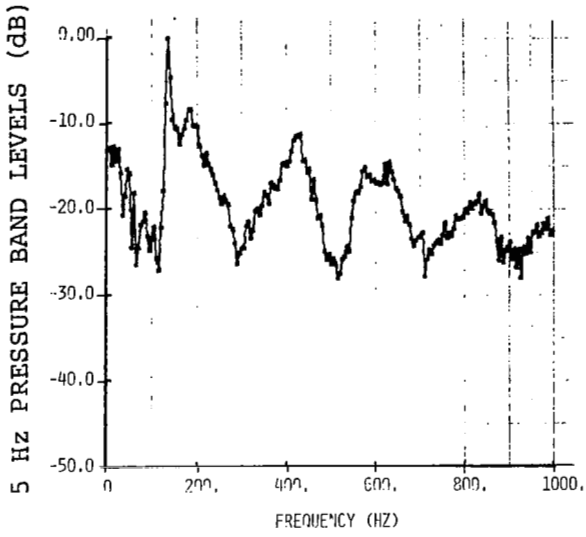

Fig. 8 Same conditions as Figs. 3-7, far field spectrum at 60° to jet axis.

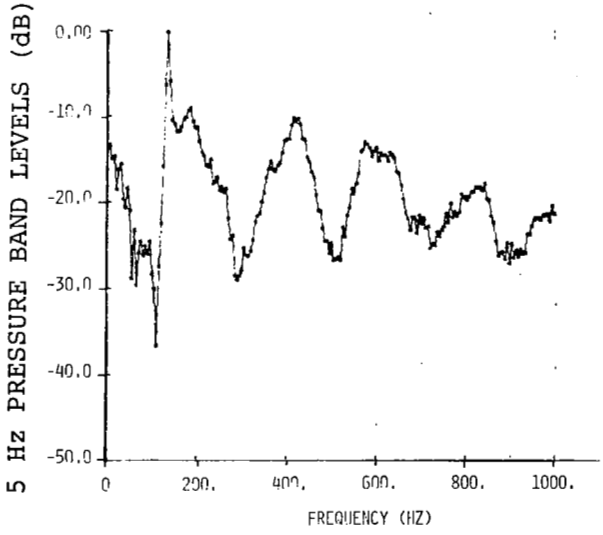

Fig. 7 Same condition as Figs. 3-6, far field spectrum at 45° to jet axis.

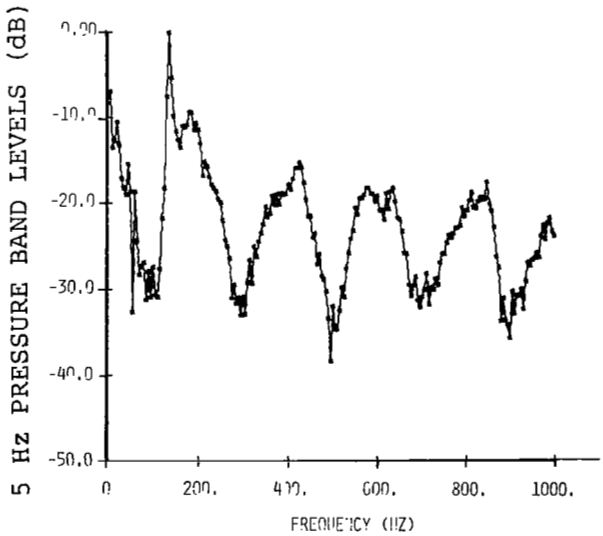

Fig. 9 Same condition as Figs. 3-8, far field spectrum at 75° to jet axis.

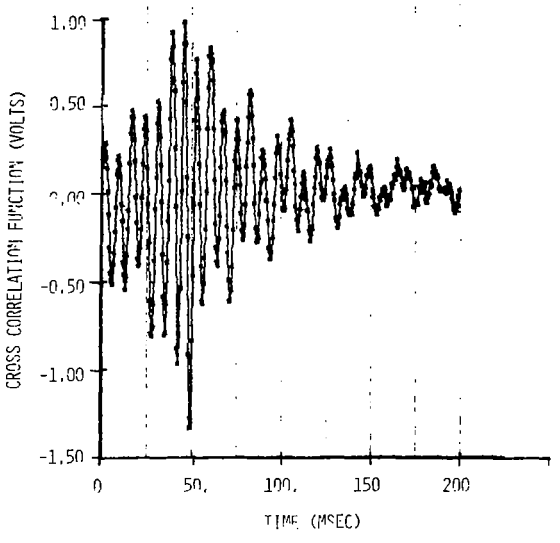

Fig. 10 Crosscorrelation of chamber pressure and far field noise (60°, 15 m), combustor 'A', air/fuel ratio 40, M_j=0.29. See Fig. 31 for normalized values of crosscorrelations.

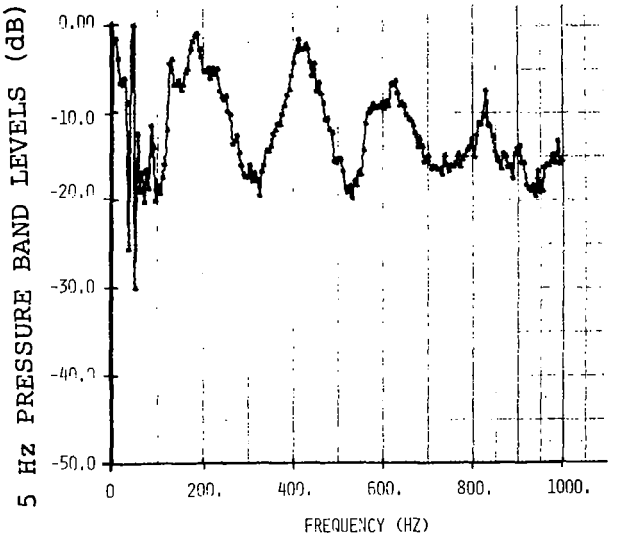

Fig. 12 Power spectral density of far field noise measured at 60° from jet axis, 15 m from the exit, as Fig. 8, but for air/fuel ratio of 50, M_j = 0.29.

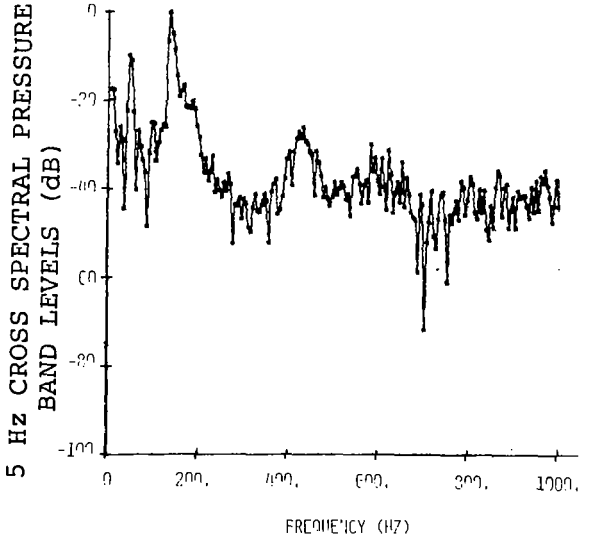

Fig. 11 Cross spectral density distribution corresponding to crosscorrelation of Fig. 10.

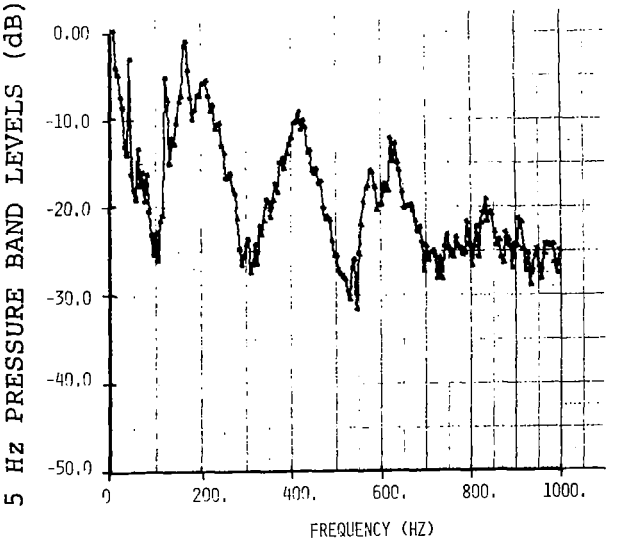

Fig. 13 Same as Fig. 12 except for air/fuel ratio of 40, M_j = 0.22.

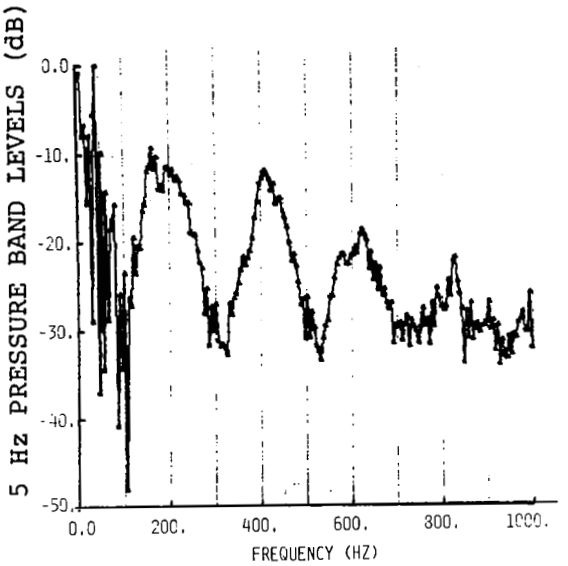

Fig. 14 Same as Figs. 12 and 13 except for air/fuel ratio of 50, M_j = 0.24.

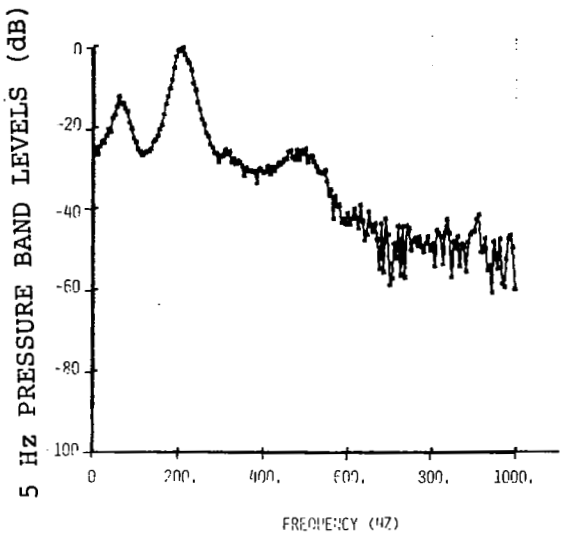

Fig. 16 Power spectral density distribution of combustion chamber pressure fluctuations, combustor 'C' air fuel ratio of 50, M_j = 0.30.

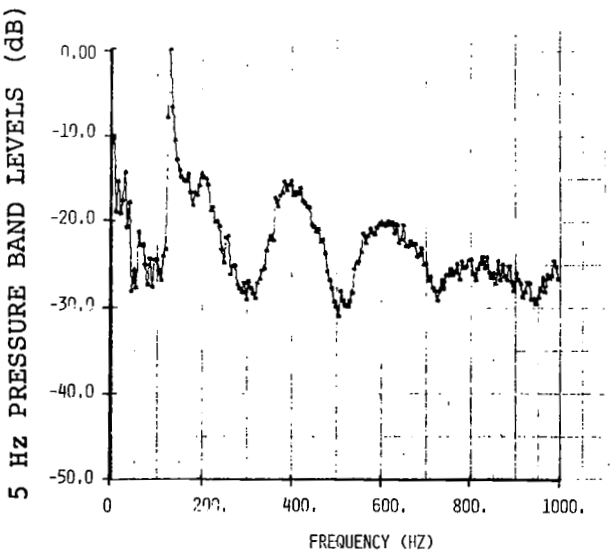

Fig. 15 Power spectral density distribution of far field noise at 60° to jet axis, combustor 'B', air/fuel ratio of 40, M_j = 0.29.

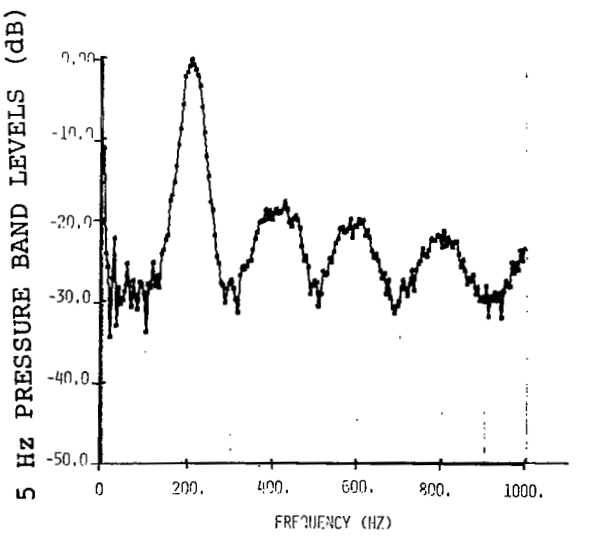

Fig. 17 Far field noise power spectral density distribution, at 60° to jet axis, combustor 'C', air/fuel ratio of 50, M_j = 0.30

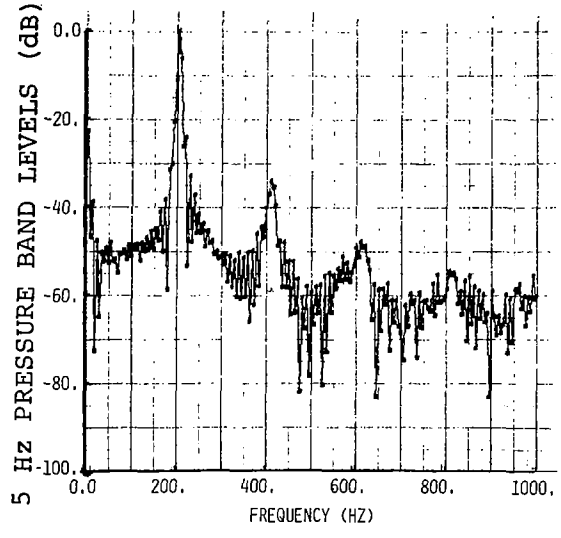

Fig. 18 As Fig. 17, except air/fuel ratio of 40, M_j = 0.24.

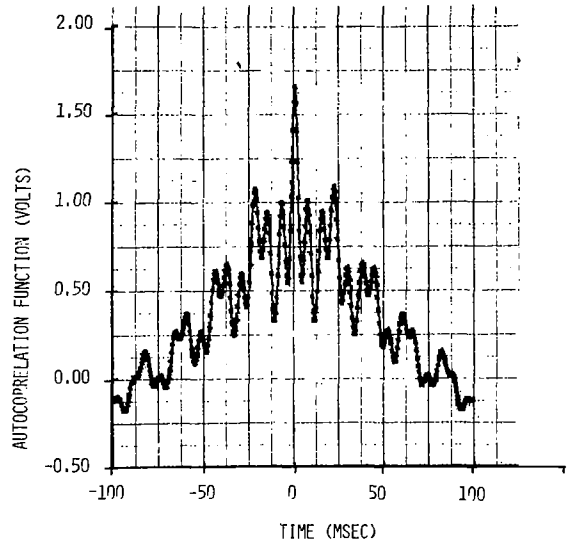

Fig. 20 Autocorrelation of combustion chamber pressure fluctuations for combustor 'A' air/fuel ratio of 40, M_j = 0.29. Spectral distribution for this case is shown in Fig. 3.

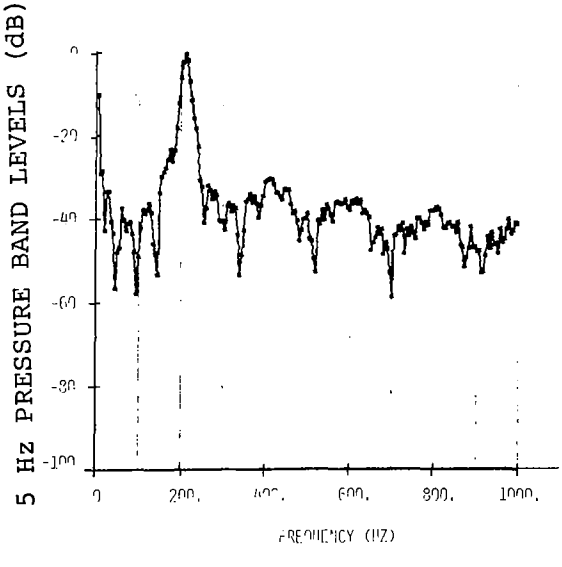

Fig. 19 As Fig. 17 and 18, except air/fuel ratio of 50, M_j = 0.25.

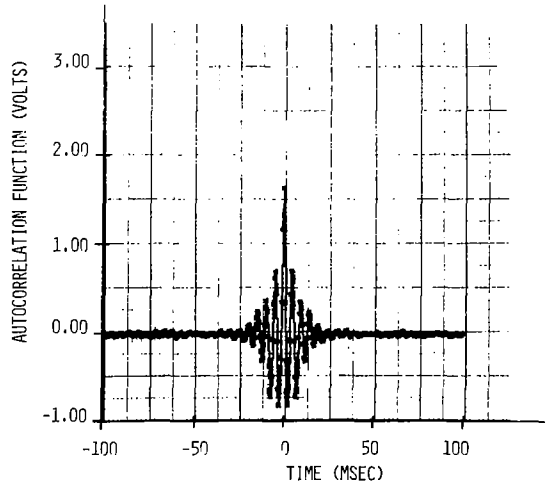

Fig. 21 Autocorrelation of combustion chamber pressure fluctuations for combustor 'C', air/fuel ratio of 50, M_j = 0.30. Spectral distribution is shown for this case in Fig. 16.

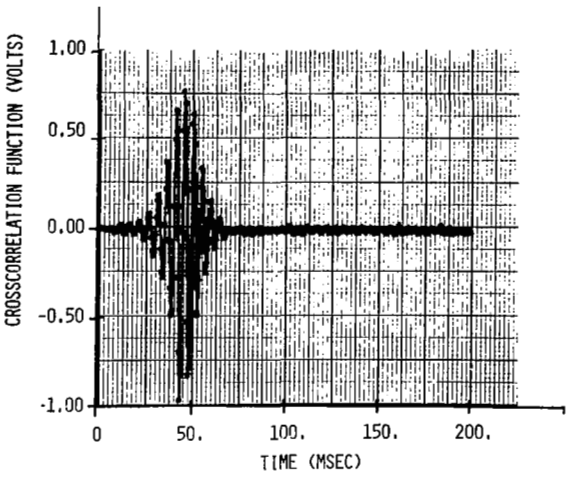

Fig. 22 Crosscorrelation between chamber pressure fluctuation and far field noise for combustor 'C' air/fuel ratio of 50, M_j = .30.

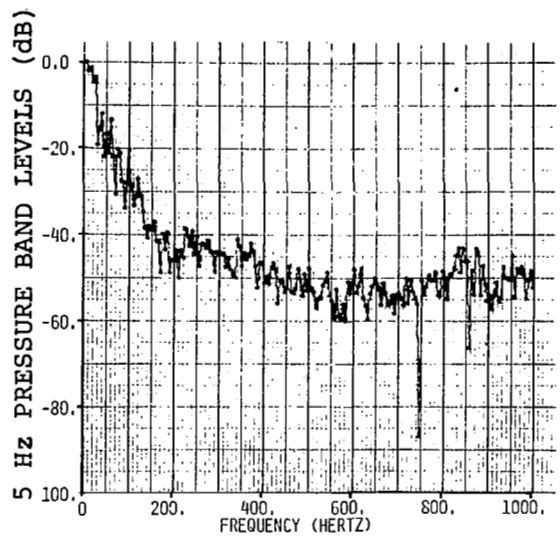

Fig. 24 Power spectral density distribution of far field noise obtained for case with ambient temperature airflow only, through combustor 'C', M_j = 0.24.

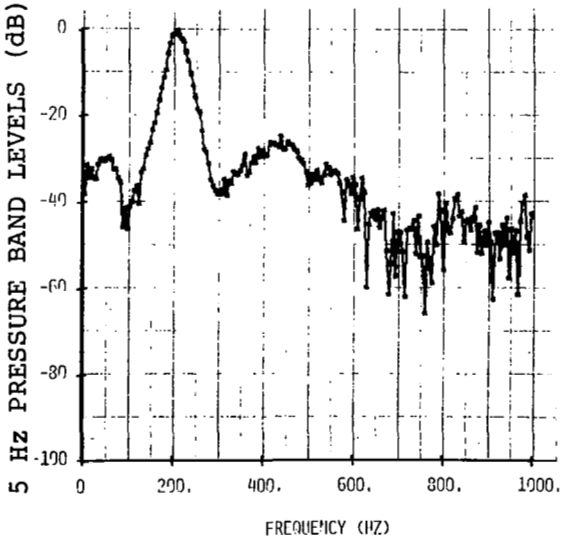

Fig. 23 Cross spectral density distribution obtained from Fig. 22.

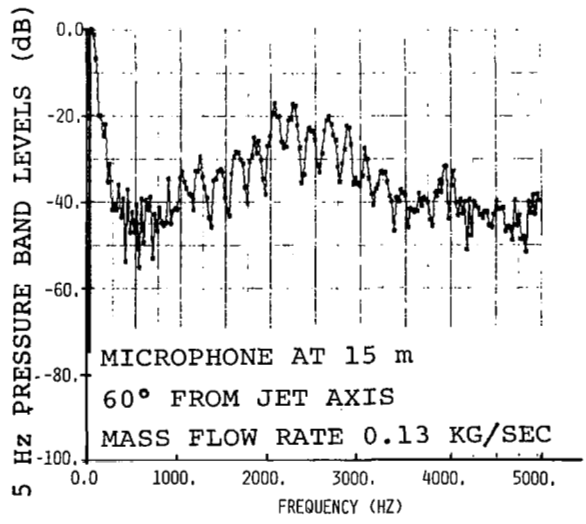

Fig. 25 Power spectral density distribution of far field noise, similar to that of Fig. 24 except that combustor can 'C' was protruding from end of duct; no combustion.

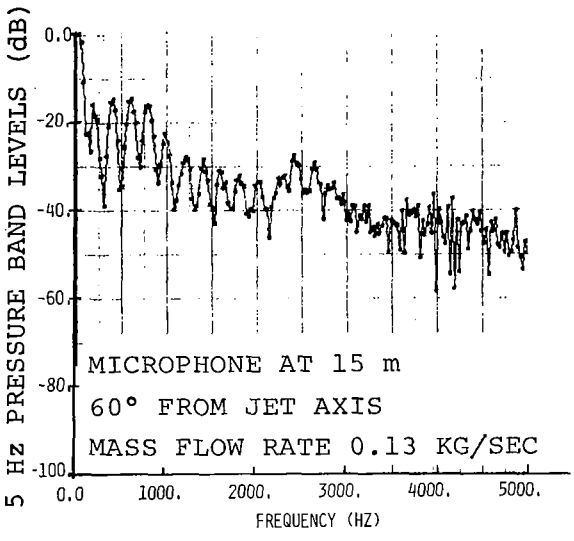

Fig. 26 Power spectral density distribution for condition as in Fig. 25, except that mixture of fuel and air was burning.

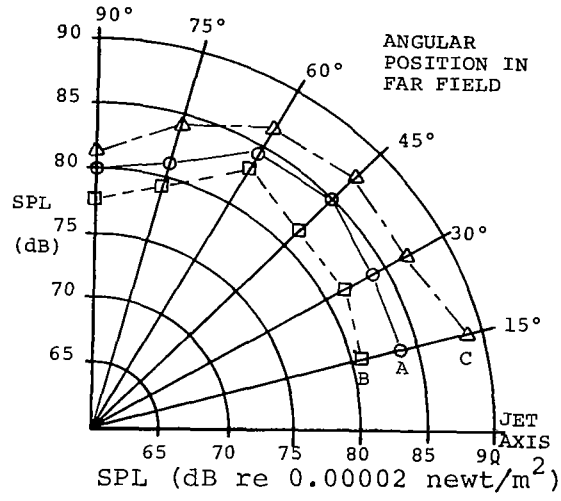

Fig. 28 Sound pressure level in far field for three combustors 'A', 'B' and 'C' at approximately the same operating conditions; air/fuel ratio = 50, M_j = 0.29.

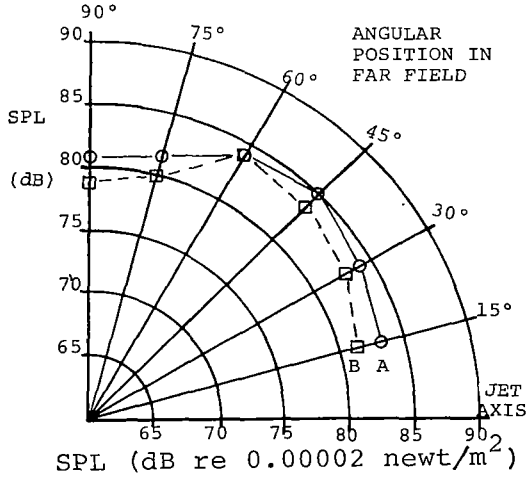

Fig. 27 Sound pressure level in far field for two combustors, 'A' and 'B', at approximately the same operating conditions; air/fuel ratio = 40, M_j = 0.29.

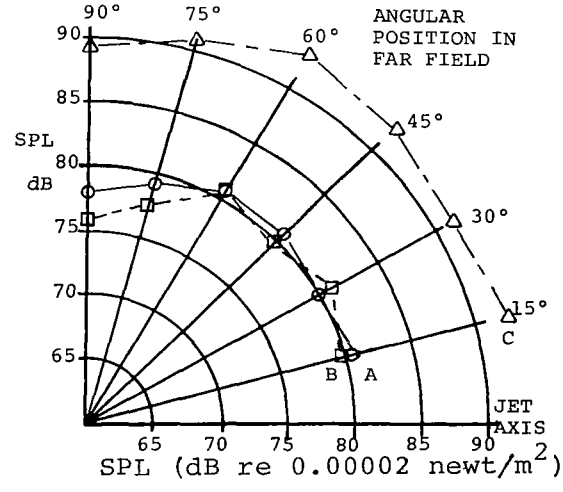

Fig. 29 Sound pressure level in far field for three combustors 'A', 'B' and 'C' at approximately the same operating conditions; air/fuel ratio = 40, M_j ≈ 0.23.

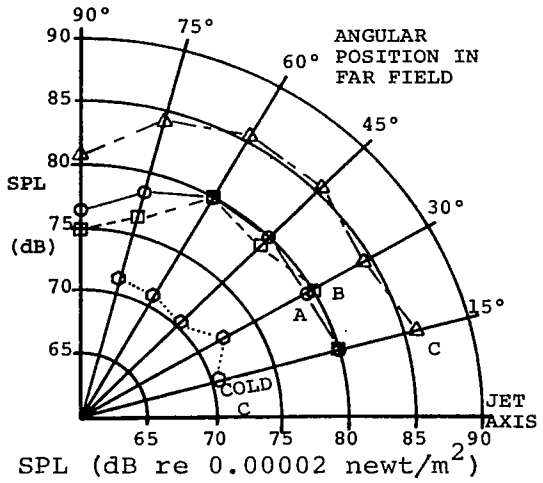

Fig. 30 Sound pressure level in far field for three combustors, 'A', 'B' and 'C' at approximately the same operating conditions; air/fuel ratio = 50, $M_j \simeq 0.25$.

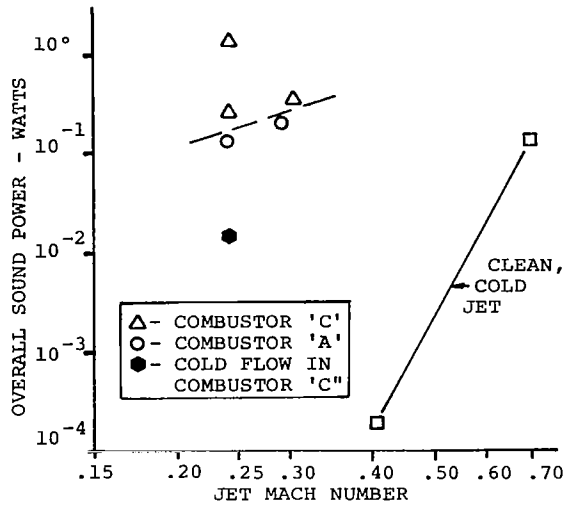

Fig. 32 Comparison of overall sound power of combustor-jet with that of an equivalent clean jet with a 5 cm dia. nozzle, using Mach number (equal thrust) as a basis of comparison.

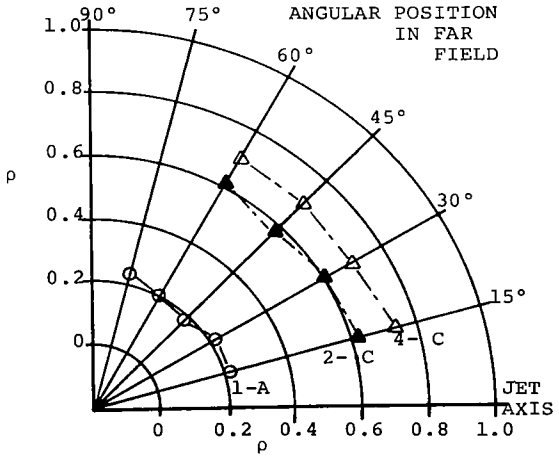

Fig. 31 Normalized crosscorrelation coefficient vs angular position in far field for three operating conditions (Table 1).

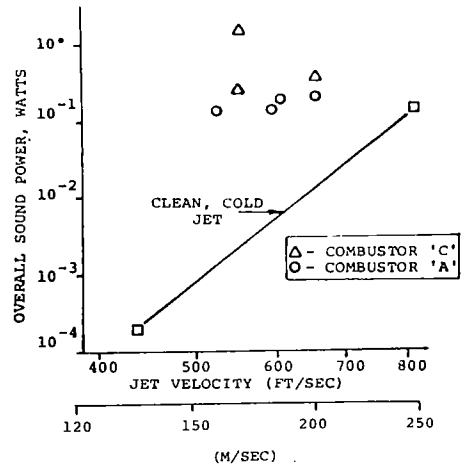

Fig. 33 Comparison of overall sound power of combustor-jet with that of an equivalent clean jet with a 5 cm dia. nozzle, using jet velocity as a basis of comparison.

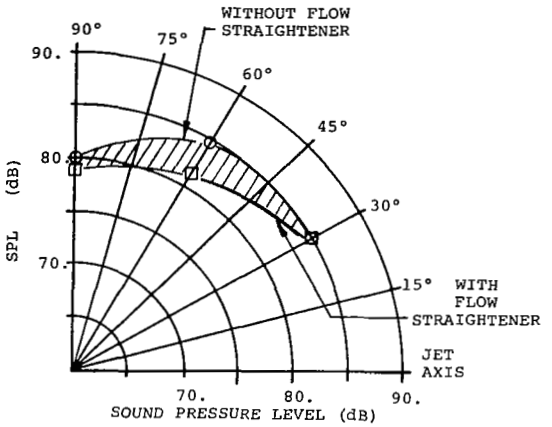

Fig. 34 Far field noise level of combustor-jet, with and without a flow straightener upstream of the exit nozzle, for an air/fuel ratio of 50, jet Mach number of 0.30, combustor 'C'.

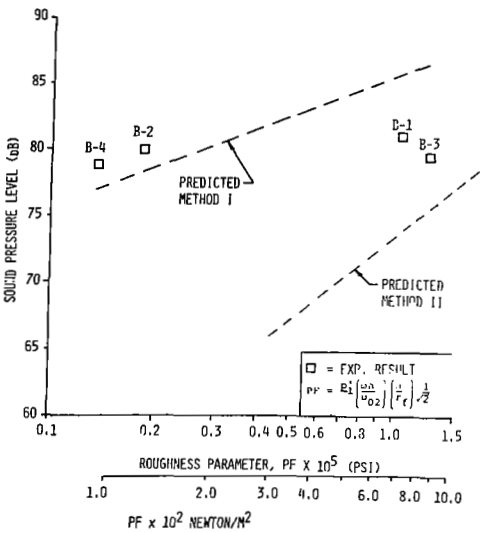

Fig. 36 Comparison as in Fig. 35, but for combustor 'B'.

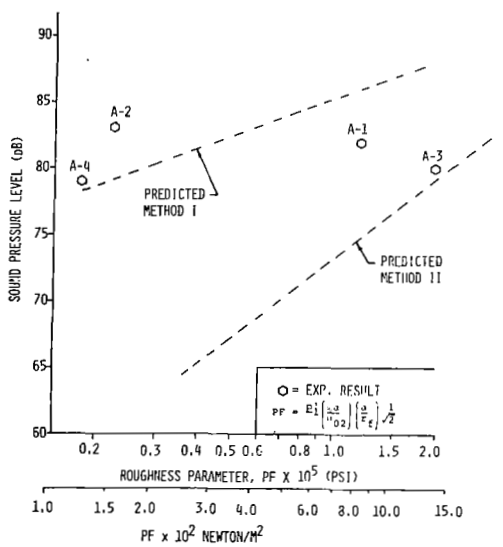

Fig. 35 Sound pressure level, combustor 'A', plotted vs the combustion roughness parameter, PF, and compared with analytically predicted levels using the two methods described in the text.

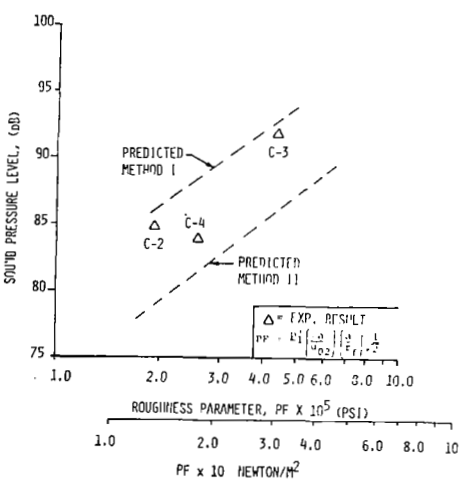

Fig. 37 Comparison as in Fig. 35, but for combustor 'C'.

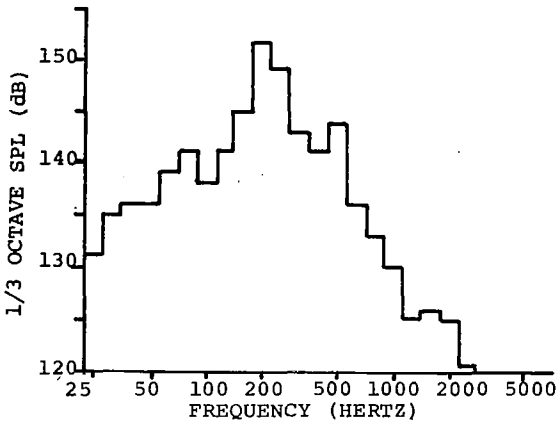

Fig. 38 1/3 Octave band pressure levels of combustor pressure fluctuations, combustor 'C', air/fuel ratio of 50, M_j = 0.30.

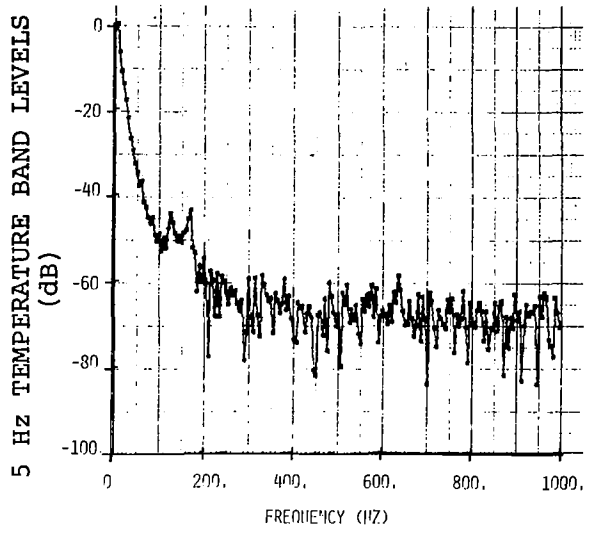

Fig. 40 Power spectral density distribution of the temperature fluctuation in the exhaust nozzle; air/fuel ratio of 70, mean temperature ≈ 1090°F.

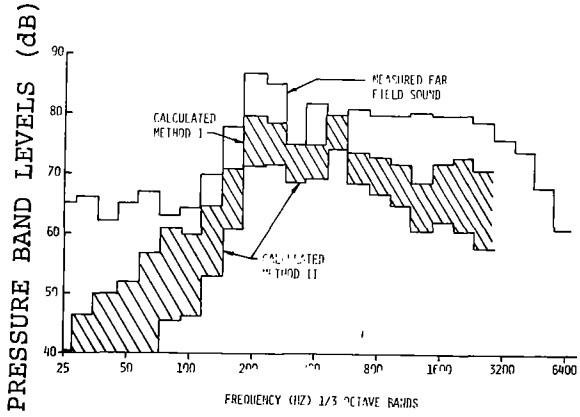

Fig. 39 Far field sound, 1/3 octave band pressure as measured, compared with levels predicted using levels in Fig. 38 together with two prediction methods described in the text.

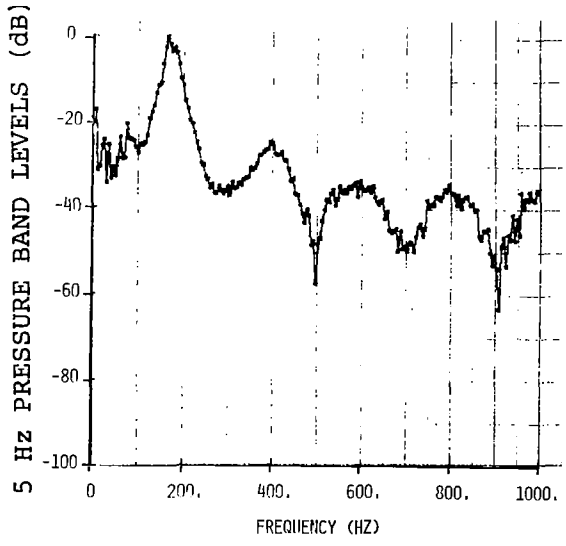

Fig. 41 Far field noise power spectral density for same case as in Fig. 40, for microphone at 60° to duct.

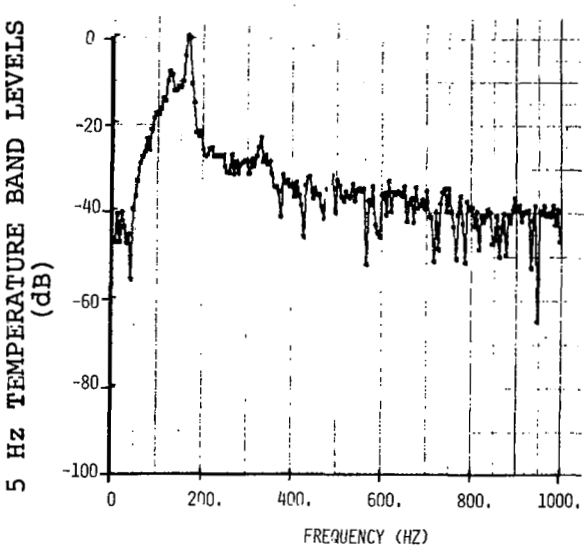

Fig. 42 Power spectral density of temperature, as Fig. 40 except that a 100 Hz highpass filter reduced the low frequency content in this record.

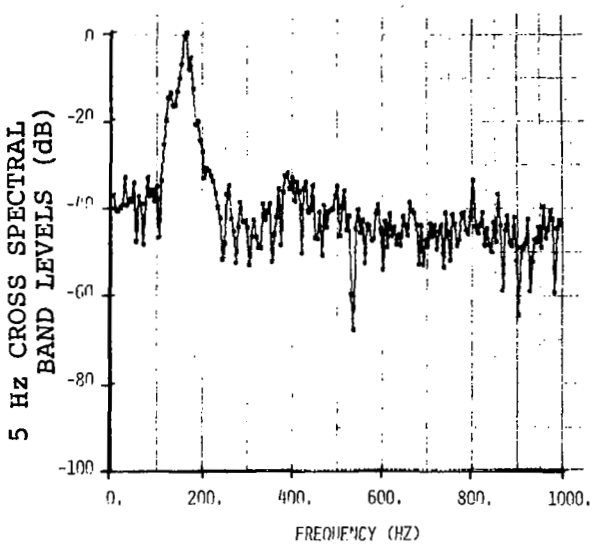

Fig. 44 Cross spectral density of nozzle temperature fluctuation and far field noise at 60° to duct axis, with 100 Hz highpass filter on each signal.

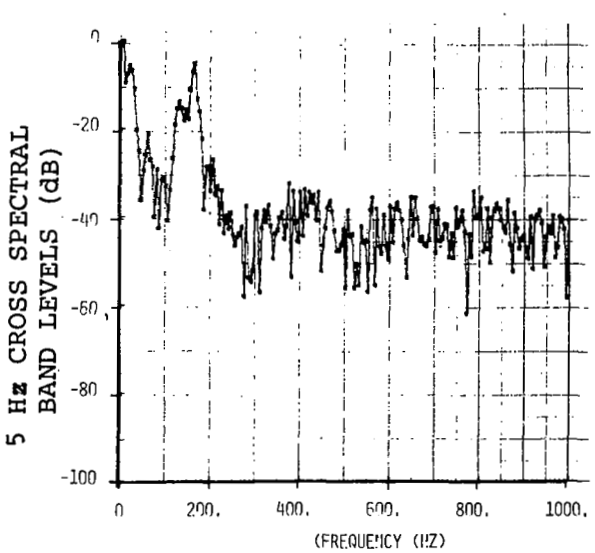

Fig. 43 Cross spectral density of nozzle temperature fluctuation and far field noise at 60° to duct axis.